Received: 13 December 2022 | Accepted: 15 December 2022

DOI: 10.1002/mawe.202200277

ARTICLE

WILEY VCH

A study on the parametric optimization of drawing metal stamping process for aluminum alloy tailgate parts using response surface methodology

Eine Studie zur Parameteroptimierung eines Metallzieh-Stanzprozesses für Heckklappenteile aus einer Aluminiumlegierung unter Verwendung der Antwort-Oberflächen-Methodik

S.-Y. Kim[1] | **B.-G. Kim**[2] | **T.-G. Lee**[3]

[1]Kongju National University, Future Automotive Intelligent Electronics Core Technology, Cheonan-si, Republic of Korea

[2]Gyeongbuk Institute of IT Convergence Industry Technology, Research and Development Division, Gyeongsan-si, Republic of Korea

[3]Samsung Tech CO., LTD., R&D Center, Gyeongsan-si, Republic of Korea

Correspondence
T.-G. Lee, Samsung Tech CO., LTD., R&D Center, Gyeongsan-si, Republic of Korea.
Email: ltg1119@naver.com

Funding information
Technology development Program, Grant/Award Number: S3055610; Ministry of SMEs and Startups (MSS, Korea); Korea Basic Science Institute (National research Facilities and Equipment Center); Ministry of Education, Grant/Award Number: 2020R1A6C101A187

Abstract

The tailgate-extension in a vehicle is a part that connects the upper and lower parts of the tailgate. Since this part does not require high strength, aluminum must be used in order to reduce the weight of the vehicle. However, when choosing aluminum, it is difficult to satisfy the shape quality with the existing manufacturing process. Therefore, this study was conducted for the purpose of optimizing the draw metal stamping process for the development of tailgate extensions for vehicles using aluminum. The response surface methodology was utilized to optimize the draw metal stamping process. The process design parameters were established as blank holding force, coefficient of friction and die speed. Finally, the reliability of the optimization process and finite element analysis was secured by conducting field experiments to review the derived optimal process conditions.

KEYWORDS
aluminum, drawing metal stamping process, optimization, tailgate

Abstract

Die Heckklappenverlängerung für Fahrzeuge ist ein Teil, das den oberen und unteren Teil der Heckklappe miteinander verbindet. Da dieses Teil keine hohe Festigkeit erfordert, kann Aluminium verwendet werden, um das Gewicht des Fahrzeugs zu verringern. Bei der Umstellung auf Aluminium ist es jedoch schwierig, die Formqualität mit dem bestehenden Herstellungsverfahren zu erreichen. Daher wurde diese Studie mit dem Ziel durchgeführt, den Prozess des Metallziehens für die Entwicklung von Heckklappenverlängerungen für Fahrzeuge aus Aluminium zu optimieren. Die Antwort-Oberflächen-Methode wurde zur Optimierung des Ziehverfahrens eingesetzt. Als

Parameter für die Prozessgestaltung wurden die Blechhaltekraft, der Reibungskoeffizient und die Werkzeuggeschwindigkeit festgelegt. Schließlich wurde die Zuverlässigkeit des Optimierungsprozesses und der finite-elemente-analyse durch die Durchführung von Versuchen zur Überprüfung der abgeleiteten optimalen Prozessbedingungen sichergestellt.

SCHLÜSSELWÖRTER
Aluminium, Heckklappe, Metallzieh-Stanzprozess, Optimierung

1 | INTRODUCTION

Recently, the development of eco-friendly vehicles to overcome environmental problems is the biggest topic in the automobile industry. In particular, an electric vehicle consisting of an electric motor and a battery has the advantage of not generating exhaust gas. However, the weight of this vehicle increases by at least 20% compared to the existing internal combustion engine vehicle due to the increase in batteries, safety devices, and convenience parts [1, 2]. Therefore, in order to improve the mileage of electric vehicles, weight reduction is essential [3–5]. One of the most common methods is to use aluminum, a lightweight material, to reduce the weight of automobiles [6–8]. However, due to the low ductility and low elastic limit of the aluminum material, there is a high possibility of problems such as cracks, burrs, wrinkle, and excessive spring-back during the forming or stamping process. In addition, since material loss is high, it is essential to improve the production process to reduce the cost burden [9, 10].

The tailgate-extension for vehicles is a part that connects the upper and lower parts of the tailgate, Figure 1. Since this part does not require high strength, aluminum must be used in order to reduce the weight of the vehicle. However, when changing the material to aluminum, it is difficult to satisfy the shape quality with the existing manufacturing process.

Therefore, this study was conducted for the purpose of optimizing the draw metal stamping process for the development of tailgate extensions for vehicles using aluminum. The response surface methodology was utilized to optimize the draw metal stamping process. The process design parameters were established as blank holding force, coefficient of friction and die speed. For optimization, a specialized tool for finite element analysis was used, and the optimization target process was set to OP10 draw. Finally, the reliability of the optimization process and finite element analysis was secured by conducting field experiments to review the derived optimal process conditions.

2 | DRAWING METAL STAMPING PROCESS FOR TAILGATE-EXTENSION PARTS

In this study, the tailgate-extension, which connects the inner panel and outer panel of the vehicle tailgate, was selected. The tailgate-extension is a part that must not be

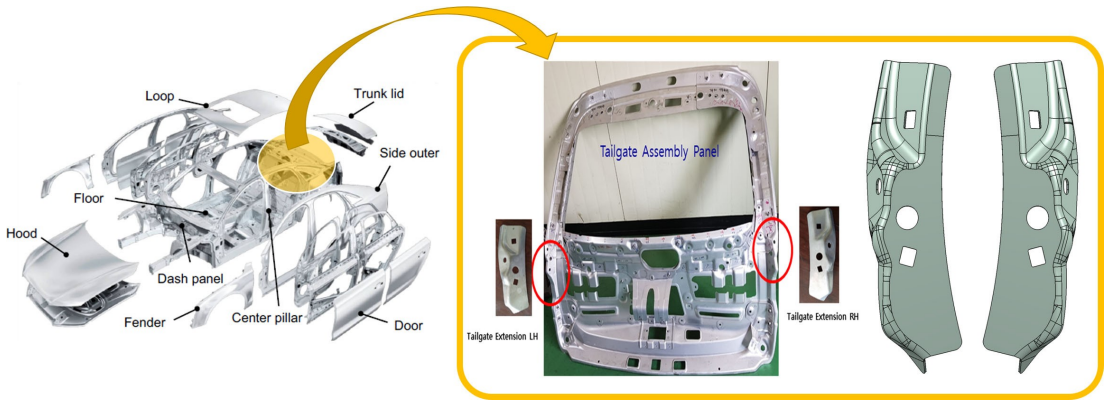

FIGURE 1 Tailgate extension parts.

BILD 1 Heckklappenverlängerungsteile.

shaken by external air resistance that rises from the front, rear, and both sides when driving a vehicle, and must have safety to absorb shocks from the outside in case of a rear-end collision. Also, as shown in Figure 1 the tailgate-extension serves to connect the two panels, so the mounting bracket and hole positions to be assembled must be accurate, and the shape accuracy of the mounting surface must be high. In general, the tailgate-extension is manufactured by a draw metal stamping process using a steel plate, but in recent years, weight reduction of parts is required, so it is a trend to change to an aluminum material. However, when changing to an aluminum material, cracks, burrs, and wrinkle occur due to low elongation and elastic limit, making it difficult to ensure quality.

3 | RESPONSE SURFACE METHODOLOGY

Response surface methodology is a method that analyzes the relationship between explanatory variables and response variables for factor analysis using an experimental design or for selection of optimal conditions. In general, the response surface methodology is used when the relationship between explanatory variables and response variables appears as a quadratic curve response, and the representative design of experiments used for this is central composite design. The central composite design has an equal prediction variance for all points that are the same distance from the centre point in all directions. In addition, at the cube point and axial point, only one experiment is performed without repetition, and repeated experiments are performed only at the centre point to obtain the error term. Therefore, when adding the axial point, it is desirable to make the variance of the response values equal by making it located at the same distance as the cube point [11–13].

The response function is usually expressed as a multiple regression model for k independent variables. A new independent variable is defined by linear transformation of the initial independent variables, and the region of interest considered by the experimenter is set as the central point. In general, it is recommended to place the independent variables between −1 and +1. Assuming that the response function is a first order regression model, it is expressed as Equation (1).

$$y = \beta_0 + \beta_1 x_1 + \cdots + \beta_k x_k \tag{1}$$

The case of the quadratic regression model is as outlined in Equation (2).

$$y = \beta_0 + \beta_1{}^* x_1 + \beta_2{}^* x_2 + \beta_3{}^* x_1 x_2 + \beta_4{}^* x_1^2 + \beta_5{}^* x_2^2 + \varepsilon \tag{2}$$

If the reaction function is a quadratic expression and the number of factors is two, the least squares estimation function can be expressed as Equation (3) with the results under various experimental conditions.

$$\hat{y} = \widehat{\beta_0} + \widehat{\beta_1} x_1 + \widehat{\beta_2} x_2 + \widehat{\beta_{11}} x_1^2 + \widehat{\beta_{22}} x_2^2 + \widehat{\beta_{12}} x_1 x_2 \tag{3}$$

The value X0, which differentiates this by x and becomes 0, is called a stationary point. Stationary points can be expressed as maximum points, minimum points, and saddle points that are neither maximum nor minimum on the secondary response surface.

4 | TEST AND FINITE ELEMENT ANALYSIS

4.1 | Tensile test

The aluminum material used in this study is an Al−Mg-Si alloy series and A6014 alloy with a thickness of 1.4 mm and T4 treatment. In order to understand the mechanical properties of A6014-T4, tensile specimens were extracted from the plates used in the actual process. For the tensile test, the standard of ISO 6892 was referenced. In order to consider the anisotropy of the plate, the specimen was extracted at angles of 0°, 45°, and 90° from the rolling direction, Figure 2. The mechanical properties of A6014-T4 were derived from tensile tests, where the swift model of Equation (4) was used for the hardening curve, Table 1 [14].

$$\sigma = K(\varepsilon_0 + \varepsilon)^n \tag{4}$$

Where K and n are the strength coefficient and strain hardening exponent, respectively. The plastic strain ratio (Lankford's value, R-value) is derived by measuring the rate of change in the thickness direction in the tensile test as in Equation (5). Normal anisotropy and planar anisotropy can be calculated from the derived R-value, and the equations for these are shown in (6) and (7) [15, 16].

$$r = \frac{\varepsilon_w}{\varepsilon_t} \tag{5}$$

$$\bar{r} = \frac{r_0 + r_{90} + 2r_{45}}{4} \tag{6}$$

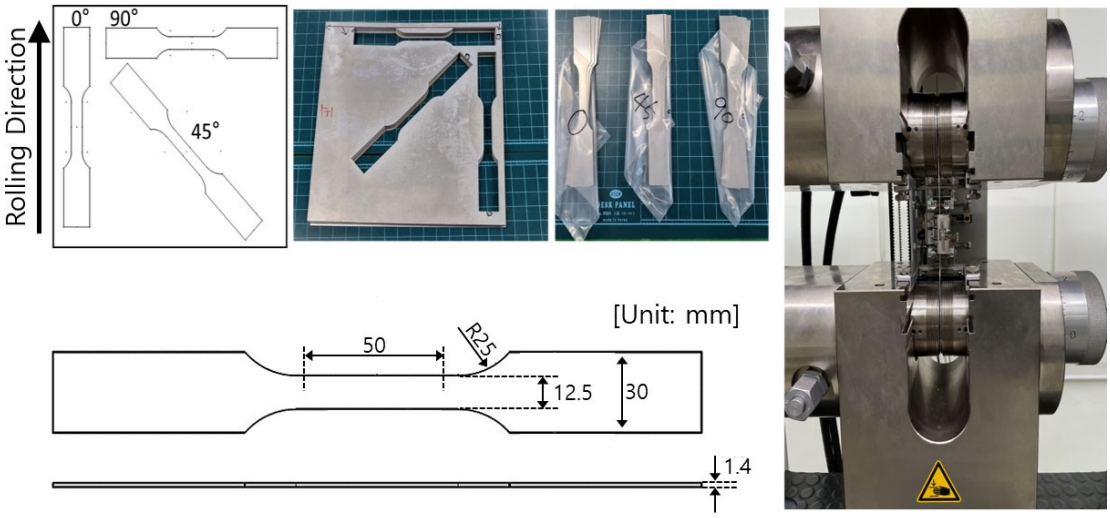

FIGURE 2 Tensile test.

BILD 2 Zugversuche.

TABLE 1 Material properties about A6014-T4(1.4 t).

TABELLE 1 Werkstoffeigenschaften A6014-T4 (1,4 t).

Parameter	Unit	Value
Density (ρ)	kg/m^3	2700
Poisson's ratio (ν)	–	0.33
Stiffness coefficient (k)	MPa	419.2033
Young's modulus (E)	GPa	69.59073
Yield strength (YS)	MPa	138.4933
Tensile strength (TS)	MPa	299.584
Strain hardening coefficient (n)	–	0.223
Plastic strain ratio (r)	–	–
Normal anisotropy ($\bar{r}$)	–	0.638
Planar anisotropy (Δr)	–	0.270
Maximum strain (ε)	%	26.5

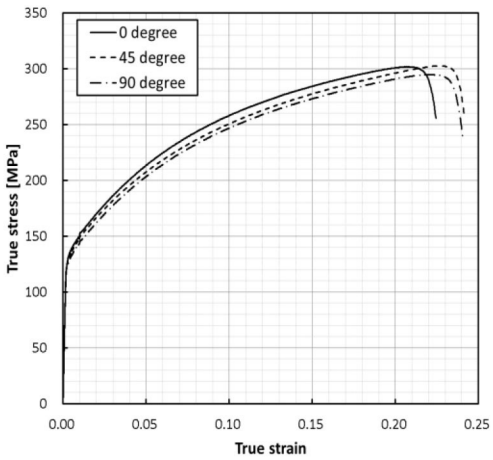

$$\Delta r = \frac{r_0 + r_{90} - 2r_{45}}{2} \tag{7}$$

4.2 | Finite element analysis models and methods

Figure 3 shows the FEM analysis model of tailgate-extension, in which four products are manufactured simultaneously with one stamping. In the draw metal stamping process in this study, the initial blank, punch, and upper die are basic elements, and a blank holder was applied to prevent excessive inflow of material. The initial blank was defined as a hexahedral element, the initial mesh size was set to 5 mm, and the mesh size after applying the adaptive mesh was set to 1.35 mm. And punch, upper die and blank holder were defined as rigid elements. The finite element analysis program was performed using Altair Hyperform and a high-performance computer aided engineering workstation (NFEC-2020-08-264228) at the Future Automotive Intelligent Electronics Core Technology Center.

4.3 | Process design variables and design of experiments

To optimize the draw metal stamping process, it is necessary to set explanatory variables and response

variables. First, in the case of explanatory variables, process design variables should be selected and then their ranges should be set. To this end, by performing a sensitivity analysis, it is possible to exclude design variables with insignificant influence of variables or reduce the range of process variables. In this study, the blank holding force, friction coefficient, and die speed were selected as explanatory variables as shown in Table 2. And among them, sensitivity analysis was performed on blank holding force. In this study, the blank holding force, friction coefficient, and die speed were selected as explanatory variables and among them, sensitivity analysis was performed on blank holding force. The sensitivity analysis was performed for setting an appropriate range of blank holding force in the draw metal stamping process. Here, the friction coefficient was set to 0.0935, and the die speed was set to 500 mm/s as in the actual manufacturing process, Table 2. The blank holding force conditions were set to 10 MPa, 5 MPa, and 2 MPa, and the sensitivity analysis results were analyzed using the forming limit diagram.

There is the forming limit diagram plot for the sensitivity analysis result, Table 3. Under the conditions of 10 MPa and 5 MPa, the failure zone occupies a high proportion in the curved part of the product, so it was found that the possibility of fracture was quite high. In the case of 2 MPa condition, there is some marginal zone, but there is no fear of breakage and it was judged as a load range in which stable forming was possible.

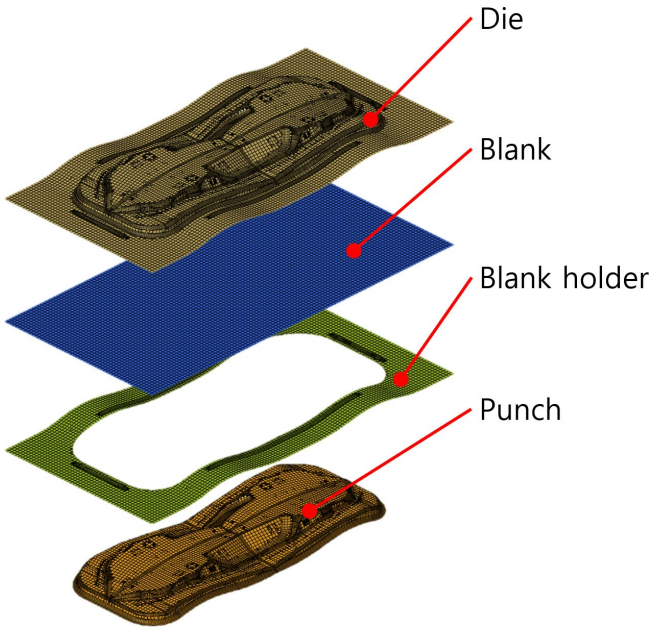

FIGURE 3 Finite element modeling for metal draw stamping.

BILD 3 Finite-Elemente-Modellierung für Metallzieh-Stanzen.

TABLE 2 Sensitivity analysis condition for blank holding force.

TABELLE 2 Bedingung der Sensitivitätsanalyse für die Haltekraft des Rohlings.

Factor		S1	S2	S3
Blank holding force	MPa	10	5	2
	N	998,253.840	499,126.922	199,650.769
Friction coefficient [μ]			0.125	
Die velocity [mm/s]			500	

TABLE 3 Sensitivity analysis result using forming limit diagram.

TABELLE 3 Ergebnis der Sensitivitätsanalyse unter Verwendung des Formgebungsgrenzdiagramms.

S1	S2	S3
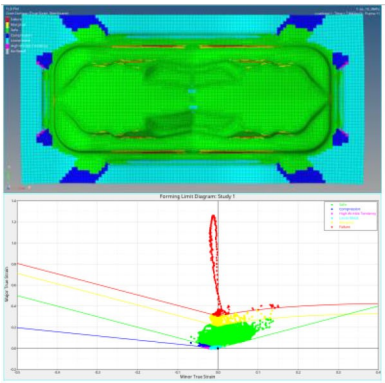	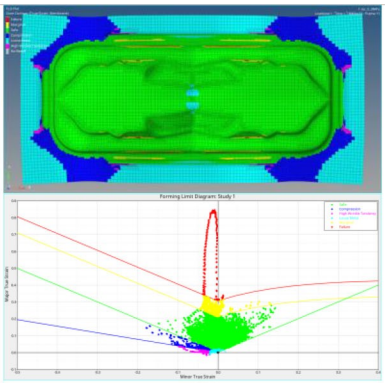	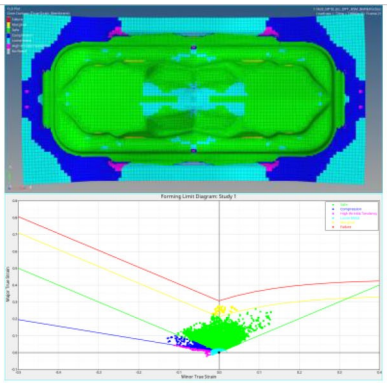

Therefore, 2 MPa was selected as a reference condition for blank holding force for process optimization. Other than that, the friction coefficient and die speed were selected in the same way as the initial conditions. Based on the reference conditions of the derived explanatory variables, values corresponding to 2-level were selected using values corresponding to 75% and 125% of the reference values of each variable. That is, three explanatory variables (blank holding force, friction coefficient, and die velocity) were selected and the level was selected as 2-level.

The orthogonal array with a central composite design was designed, Table 4. Here, replicated conditions were excluded, and the response value (y) was selected as the maximum stress and thickness reduction rate. This is because thickness reduction due to high tensile stress in drawing forming is the main cause of fracture. The characteristics of the desirability function for the response value were set as smaller-the-better characteristics.

TABLE 4 Central composite design orthogonal array.

TABELLE 4 Zentrales orthogonales Verbunddesignfeld.

Std. order	Blank holding force [MPa]	Friction coefficient [−]	Die velocity [mm/s]
1	1.500	0.094	375.00
2	2.500	0.094	375.00
3	1.500	0.156	375.00
4	2.500	0.156	375.00
5	1.500	0.094	625.00
6	2.500	0.094	625.00
7	1.500	0.156	625.00
8	2.500	0.156	625.00
9	1.159	0.125	500.00
10	2.841	0.125	500.00
11	2.000	0.072	500.00
12	2.000	0.178	500.00
13	2.000	0.125	289.75
14	2.000	0.125	710.25
15	2.000	0.125	500.00

4.4 | Analysis results and optimization

Table 5 shows the results of FEM analysis using the central composite design. The response variables were set to thinning and maximum stress, and the response values were standardized to follow a standard normal distribution with a mean of 0 and a standard deviation of 1 to increase the accuracy of data analysis, Table 5.

First, all of the second-order interaction terms were analyzed as insignificant through Student's t-test, so they were pooled in the error term, and the results are shown in Table 6.

Next, in the main effect, it was found that the die velocity was not significant as a variable for process optimization as it was out of the significance level. However,

TABLE 5 Result of finite element analysis.

TABELLE 5 Ergebnis der Finite-Elemente-Analyse.

Std. order	Blank holding force [MPa]	Friction coefficient [−]	Die velocity [mm/s]	Thinning [−]	Max. stress [−]
1	1.500	0.094	375.00	−1.364	−3.726
2	2.500	0.094	375.00	−0.132	0.591
3	1.500	0.156	375.00	−0.421	−0.562
4	2.500	0.156	375.00	1.807	0.159
5	1.500	0.094	625.00	−1.364	−0.427
6	2.500	0.094	625.00	−0.159	0.375
7	1.500	0.156	625.00	−0.421	−0.640
8	2.500	0.156	625.00	1.833	0.131
9	1.159	0.125	500.00	−1.548	−0.669
10	2.841	0.125	500.00	0.785	−0.027
11	2.000	0.072	500.00	−0.919	−0.362
12	2.000	0.178	500.00	2.096	0.268
13	2.000	0.125	289.75	−0.001	0.690
14	2.000	0.125	710.25	−0.028	0.433
15	2.000	0.125	500.00	−0.028	0.627

in the actual process, as the die velocity increases, the output increases, so it is a very important parameter. Therefore, the die speed was not pooled into the error term.

Finally, analysis of variance was performed to examine the validity of the response variables and the reliability of the regression model, Table 7.

As a result, the adjusted R square was thinning 94.56% and maximum stress 73.81%, confirming the validity of the response variable and the reliability of the regression model. The regression models derived through this are shown in the following Equations (8) and (9).

$$\begin{aligned} Thinning = {} & -1.4239 + 1.848(B.H.F) - \\ & 0.580883(Friction) - 0.000026(Velocity) - \\ & 0.576066(B.H.F \cdot B.H.F) + 0.020355(Friction \cdot Friction) \\ & +0.163559(BHF \cdot Friction) \end{aligned} \tag{8}$$

$$\begin{aligned} Max.\ stress = {} & -22.5214 + 15.24(B.H.F) + 1.25(Friction) - \\ & 0.001273(Velocity) - 2.796(B.H.F \cdot B.H.F) - \\ & 0.03665(Friction \cdot Friction) - 0.212506(B.H.F \cdot Friction) \end{aligned} \tag{9}$$

3D contour plots and optimization results for the response variable values are presented, Figure 4. In

TABLE 6 Estimation of the second-order response surface parameters (coded unit).

TABELLE 6 Abschätzung der Antwort-Oberflächen-Parameter zweiter Ordnung (codierte Einheit).

	Thinning				Max. stress			
Parameter	**Estimate**	**Std. error**	**T-value**	**P-value**	**Estimate**	**Std. error**	**T-value**	**P-value**
Constant	−0.037	0.046	−0.818	0.428	0.722	0.120	6.017	0.000
B.H.F	0.794	0.036	22.226	0.000	0.701	0.094	7.474	0.000
Friction	0.797	0.036	22.319	0.000	−0.286	0.094	−3.054	0.009
Die velocity	−0.003	0.036	−0.090	0.929	−0.159	0.094	−1.697	0.114
B.H.F · B.H.F	−0.144	0.035	−4.163	0.001	−0.699	0.091	−7.698	0.000
Friction · Friction	0.199	0.035	5.746	0.000	−0.358	0.091	−3.942	0.002

TABLE 7 Analysis of variance about thinning and maximum stress.

TABELLE 7 Varianzanalyse bezüglich Dickenabnahme und maximaler Spannung.

Thinning					
	d.f	**Sum of square**	**Mean square**	**F-value**	**P-value**
Regression	6	18.773	3.129	179.541	0.000
Residual	13	0.227	0.017	–	–
Lack of fit	8	0.227	0.028	–	–
Pure error	5	0.000	–	–	–
Total	19	19.000	1.000	–	–
	s	R-sq	R-sq(adj)	R-sq(Pred)	Adeq Precision
	0.132	98.81%	98.26%	94.56%	46.704
Max.stress					
	d.f	**Sum of square**	**Mean square**	**F-value**	**P-value**
Regression	6	18.773	3.129	179.541	0.000
Residual	13	0.227	0.017	–	–
Lack of fit	8	0.227	0.028	–	–
Pure error	5	0.000	–	–	–
Total	19	19.000	1.000	–	–
	s	R-sq	R-sq(adj)	R-sq(Pred)	Adeq precision
	0.3464	91.79%	88.00%	73.81%	17.452

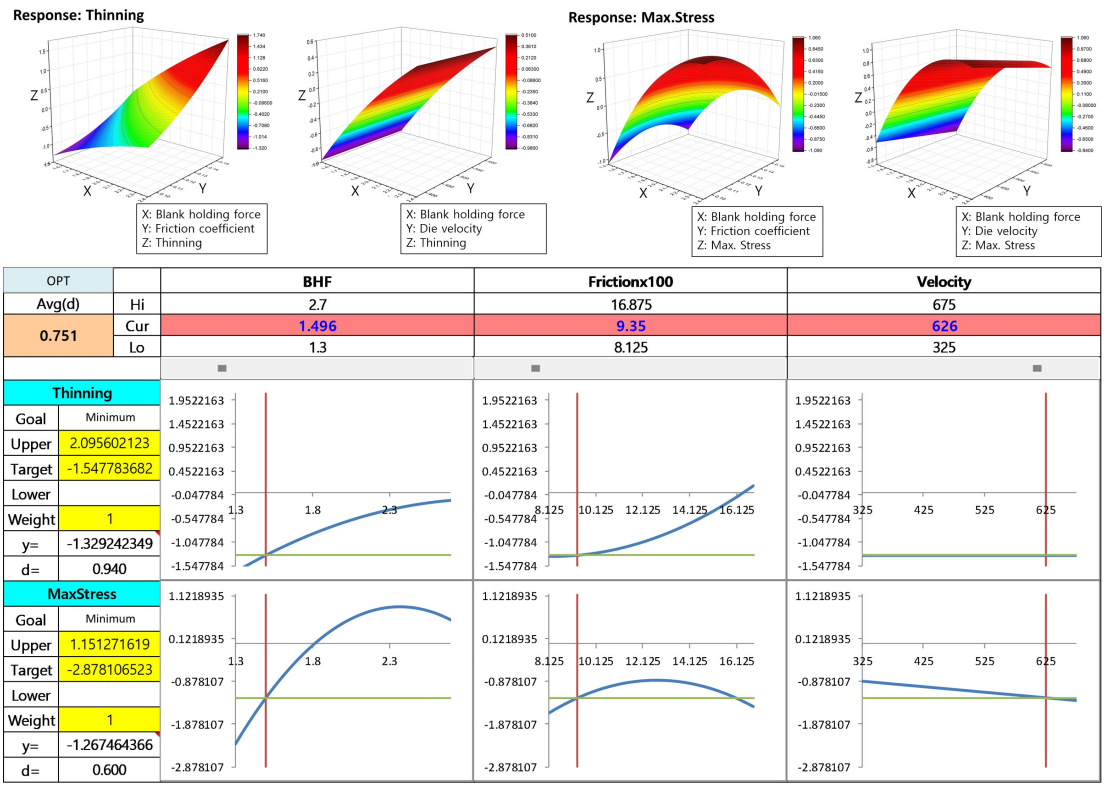

FIGURE 4 Analysis results of optimum condition.

BILD 4 Analyseergebnis des optimalen Zustands.

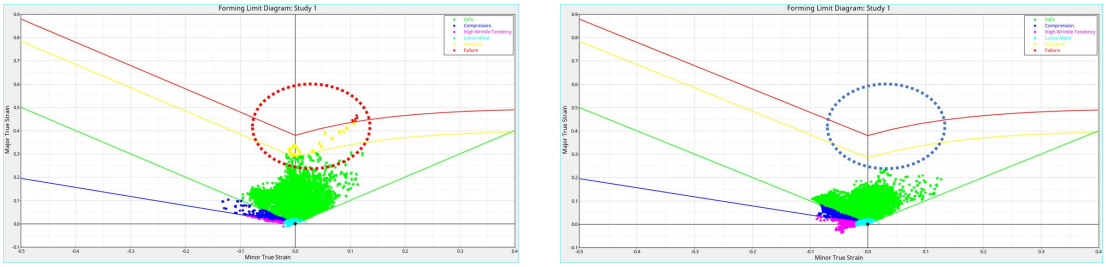

FIGURE 5 Comparison of forming limit diagram curves before and after optimization (left: before, right: after).

BILD 5 Vergleich der Grenzformänderungsschaubildkurven vor und nach der Optimierung (links: vorher, rechts: nachher).

thinning, both blank holding force and coefficient tended to decrease as the values decreased. However, it was found that there was no effect according to the change of the die velocity. In the maximum stress, the blank holding force and friction coefficient appeared in the form of quadratic functions with negative coefficients. In the case of the die velocity, it was confirmed as a tendency inversely proportional to the maximum stress as it appeared in the form of a linear function with a negative slope. Finally, the optimal conditions selected were a blank holding force of 1.496 MPa, a friction coefficient of 0.0935, and a die velocity of 626 mm/s. Comparing before and after optimization, and it was confirmed that the failure zone and marginal zone disappeared from the forming limit diagram curve, Figure 5. However, the high wrinkle tendency zone showed a slight increase, but this was confirmed as the blank holder area, and it was judged that there was no effect on the formability of the product.

In order to analytically verify the derived optimization conditions, data compared with analysis results under similar conditions were extracted, Table 8. In the case of blank holding force, it was set as a fixed condition because it was a variable that went through both sensitivity analysis and optimization analysis. For the coefficient of friction, 0.094, which is the optimal condition, and 0.156, which corresponds to 125% of the reference value, were selected. Lastly, since the die velocity

TABLE 8 Case study result for optimum condition verification.

TABELLE 8 Ergebnis der Fallstudie zur Überprüfung der optimalen Bedingung.

Case	Blank holding force [MPa]	Friction coefficient [−]	Die velocity [mm/s]	Thinning [%]	Max. stress [MPa]
Optimum	1.496	0.094	626	25.21	418.707
Case 1			500	25.21	422.572
Case 2		0.156	626	27.86	409.815
Case 3			500	27.86	406.991

TABLE 9 Forming limit diagram (FLD) zone ratio results.

TABELLE 9 Ergebnisse für das Grenzformänderungsschaubild Zonenverhältnis.

FLD zone	Optimum [%]	Case 1 [%]	Case 2 [%]	Case 3 [%]
Safe	73.40	73.30	78.70	78.80
Compression	9.30	9.60	8.00	8.00
High wrinkle tendency	3.20	3.20	2.30	2.30
Loose metal	14.10	13.90	11.00	10.90
Marginal	0.00	0.00	0.00	0.00
Failure	0.00	0.00	0.00	0.00

was a statistically insignificant factor, 626 mm/s and 500 mm/s were selected for comparison between the optimal and reference conditions.

First, in the case of the die velocity, there was no effect on the thickness reduction rate according to the increase of the velocity, and the maximum stress showed a tendency to decrease. However, its influence was also judged to be insignificant. In the trend of decreasing maximum stress, the difference between optimum and case 1 was about 3.8 MPa, so the effect was also judged to be insignificant.

Next, the effect of the friction coefficient was clearly shown in the thickness reduction rate. Comparing the optimum and case 2, as the friction coefficient increased, the thickness reduction rate also increased, showing a difference of about 2.65%. The maximum stress showed a tendency to decrease as the friction coefficient increased, and the difference was about 8.9 MPa. This was judged as a result of proving that the die velocity was not significant in the previously performed analysis of variance.

Third, the results were derived by comparing the forming limit diagram, Table 9. As the friction coefficient increased, the safe zone increased, the compression zone decreased, the high wrinkle tension zone decreased, the loose metal zone decreased, the material thickness decreased, and the maximum stress increased.

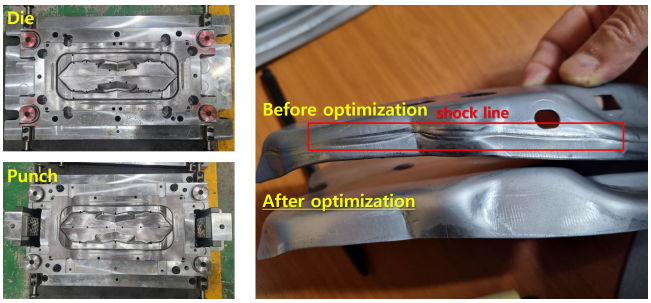

FIGURE 6 Comparison of formability before and after optimization through field experiments.

BILD 6 Vergleich der Umformbarkeit vor und nach der Optimierung durch Versuche.

Among them, in the case of the high wrinkle tendency zone, tailgate parts were not affected in all analysis conditions. In conclusion, it was confirmed that the reduction rate of the material thickness was the most important optimization condition, and it was confirmed that the process condition derived from the optimization was the most ideal condition.

Finally, the past process conditions manufactured with steel materials and the process conditions optimized for aluminum materials were applied to the actual field and compared, Figure 6. As a result, in the existing process, a shock line was generated at the position where the die and the blank holder were in contact,

whereas it was confirmed that the forming was perfect without the occurrence of a shock line in the optimized process condition.

5 | CONCLUSIONS

This study was conducted for the purpose of optimizing the draw metal stamping process for the development of tailgate extensions for vehicles using aluminum. To this end, an orthogonal array was constructed to utilize the response surface methodology, and the following conclusions were drawn by analyzing the results of finite element analysis and experiments.

1. The range of explanatory variables was set based on the process conditions of tailgate-extension parts manufactured from steel plates. Setting the range of explanatory variables could reduce the optimization range by performing sensitivity analysis. Based on this, it was possible to construct an orthogonal array to which the central composite design was applied.
2. In order to consider the anisotropy of the aluminum material, a tensile test was performed by extracting specimens at angles of 0°, 45°, and 90° from the rolling direction. The plastic strain ratio (Lankford's value, R-value) was derived by measuring the thickness variation of the tensile test specimen. Using this, normal anisotropy and planar anisotropy were calculated, and the accuracy of sheet metal forming analysis could be improved by applying it to finite element analysis.
3. finite element analysis was performed using an orthogonal array to which a central composite design was applied. As a result of this, it was confirmed that all second-order interactions were not significant through analysis of variance. In addition, it was confirmed that the die velocity deviates from the significance level in the main effect.
4. The thickness of the aluminum material showed a tendency to be inversely proportional to the blank holding force and friction coefficient. Since these are factors that prevent material from flowing into the die, it was confirmed that excessive force and friction coefficient act as decisive factors for reducing the thickness of the material. However, it was found that the die velocity did not affect the thickness change of the material. Since the design of experiment was established in consideration of the range of the adjustable die velocity in the actual process, it was determined that the velocity range was notsufficient to affect the thickness reduction of the material.
5. In order to verify the optimal process conditions derived from finite element analysis, a case study using finite element analysis and actual field experiments were conducted. Through this, it was confirmed that the formability was clearly improved compared to the previous process conditions. However, dimensional accuracy, shape accuracy, and spring-back have not yet been verified, so it is judged that additional research is needed.

ACKNOWLEDGEMENTS

This work was supported by the Technology development Program (S3055610) funded by the Ministry of SMEs and Startups (MSS, Korea). This research was also supported by Korea Basic Science Institute (National research Facilities and Equipment Center) grant funded by the Ministry of Education (2020R1A6C101A187).

ORCID

S.-Y. Kim http://orcid.org/0000-0001-7124-9207

REFERENCES

1. D. P. Francesco, L. Berzi, A. Antonacci, M. Delogu, *Machines* **2020**, *8*, 1.
2. Y. D. Chung, H. Kang, W. S. Cho, presented at *Seoul 2000 FISITA World Automotive Congress*, Seoul, Korea, June 12, **2000**, pp. 1–4.
3. S. Wenlong, C. Xiaokai, W. Lu, *Ener. Proc.* **2016**, *88*, 889.
4. Z. G. Zhu, *J. Light Metals* **2011**, *10*, 3.
5. R. Smerd, S. Winkler, C. Salisbury, M. Worswick, D. Lloyd, M. Finn, *Int. J. Imp. Eng.* **2005**, *32*, 541.
6. E. P. Kwon, H. K. Park, *J. Kor. Soc. Mech. Tech.* **2018**, *20*, 886.
7. Y. S. Kim, S. H. Yang, *Chin. J. Mech. Eng.* **2017**, *30*, 625.
8. S. L. Han, Q. L. Zeng, C. Lin, Y. Gao, Y. F. Jia, *Int. J. Ad.v Man. Tech.* **2014**, *70*, 701.
9. S. H. Kim, *JKSPE* **2011**, *28*, 496.
10. C. I. Kim, S. H. Yang, Y. S. Kim, *Tran. KSME, A* **2012**, *36*, 179.
11. P. Krajnik, J. Kopac, A. Sluga, *J Mat. Proc. Tech.* **2005**, *162*, 629.
12. I. Kaymaz, C. A. McMahon, *Prob. Eng. Mech.* **2005**, *20*, 11.
13. G. Gary Wang, Z. Dong, P. Aitchison, *Eng. Opt.* **2001**, *33*, 707.
14. M. C. Butuc, C. Teodosiu, F. Barlat, J. J. Gracio, *Eur. J. Mech. A. Sol.* **2011**, *30*, 532.
15. S. Kodukula, T. Manninen, D. Porter, *ISIJ Int.* **2021**, *61*, 401.
16. B. Hutchinson, *Mat. Sci. Tech.* **2015**, *31*, 1393.

How to cite this article: S.-Y. Kim, B.-G. Kim, T.-G. Lee, *Materialwiss. Werkstofftech.* **2023**, *54*, e202200277. https://doi.org/10.1002/mawe.202200277